

A transient variable 6 Hz QPO from GX 339-4

E. Nespoli^{1,2}, T. Belloni¹, J. Homan¹, J.M. Miller³, W.H.G Lewin⁴, M. Méndez⁵, and M. van der Klis⁶

¹ INAF – Osservatorio Astronomico di Brera, Via E. Bianchi 46, I-23807 Merate (LC), Italy

² Università degli Studi di Milano, Via Celoria 16, I-20133, Milano, Italy

³ Harvard-Smithsonian Center for Astrophysics, 60 Garden Street, Cambridge, MA 02138, USA

⁴ Center for Space Research, Massachusetts Institute of Technology, 77 Massachusetts Avenue, Cambridge, MA 02139-4307, USA

⁵ SRON National Institute for Space Research, Sorbonnelaan 2, 3584 CA Utrecht, the Netherlands

⁶ Astronomical Institute “Anton Pannekoek” University of Amsterdam and Center for High-Energy Astrophysics, Kruislaan 403, NL 1098 SJ Amsterdam, Netherlands.

Received ???; accepted ???

Abstract. We report the results of an observation with the Rossi X-ray Timing Explorer of the black hole candidate GX 339-4 during its 2002/2003 outburst. This observation took place during a spectral transition from the hard to the soft state. A strong (6% rms) transient quasi-periodic oscillation (QPO) appears suddenly in the power density spectrum during this observation. The QPO centroid is ~ 6 Hz, but it varies significantly between 5 and 7 Hz with a characteristic time scale of ~ 10 seconds, correlated with the 2-30 keV count rate. The appearance of the QPO is related to spectral hardening of the flux, due to a change in the relative contribution of the soft and hard spectral components. We compare this peculiar behavior with results from other systems that show similar low frequency QPO peaks, and discuss the results in terms of possible theoretical models for QPO production.

Key words. accretion: accretion disks – black hole physics – stars: oscillations – X-rays: stars

1. Introduction

Variability studies of black-hole candidates (BHCs) have revealed the presence of many types of quasi-periodic oscillations (QPOs) in the X-ray flux of these systems (van der Klis 1995; Remillard et al. 2002a). While most BHC have shown QPOs between 0.01 and 30 Hz, in several of them also QPOs above 40 Hz have been detected. In particular, QPOs between 1 and 10 Hz are very common in these systems and are probably linked to similar features in neutron star systems (Belloni et al. 2002b). As both the low and high frequency QPOs are thought to arise in the accretion flow close to the black hole, they are a potentially important tool in determining the properties of these compact objects and the accretion flow.

The presence and the properties of QPOs in BHCs seems to be related to the spectral characteristics of the source. In this respect, transient BHCs are particularly important for the study of QPOs, since these systems show outbursts during which the mass accretion rate changes by several orders of magnitude, usually resulting in several transitions between different accretion modes or states. These states are characterized by distinct spectral and temporal properties. QPOs are mostly found in states in

which the hard spectral component contributes significantly to the spectrum and they are usually stronger at higher energies. Although a considerable amount of data showing QPOs has been collected over the years, many issues such as the nature of the frequency changes, appearance/disappearance of the QPOs, relation to less coherent variability, etc., have remained unsolved. Several theoretical models exist for these oscillations, but there is no consensus as to their physical nature (Alpar & Shaham 1985; Strohmayer et al. 1996; Miller et al. 1998; Stella & Vietri 1998).

GX 339-4, for which the recently established mass function ($5.8 \pm 0.5 M_{\odot}$, Hynes et al. 2003) indicates the presence of a black-hole primary, is usually referred to as a persistent BHC. However, its long term behavior is more similar to that of transients and it is one of the few sources that has shown all black hole spectral/timing states (see Tanaka & Lewin 1995; Homan et al. 2001; Nowak 2002, for a detailed description of black hole states). While GX 339-4 is usually observed in the low/hard state (LS), several state-transitions have been reported (Maejima et al. 1984; Miyamoto et al. 1991; Belloni et al. 1999). Strong QPOs were observed in the power density spectra of GX 339-4 during its state transitions. Miyamoto et al. (1991) reported 1-15 Hz QPO together with strong variable band-limited noise in the VHS tran-

sition observed with Ginga. A complete analysis of similar oscillations in the transient GS 1124-68 was performed by Takizawa et al. (1997), who showed that there are two different sets of QPOs, with different dependence on the source count rate. During these observations, fast count rate variations were observed, coinciding with changes in the spectral and timing properties (Miyamoto et al. 1991; Takizawa et al. 1997). So far, no high frequency QPOs have been detected in GX 339-4.

After its 1998/1999 outburst, GX 339-4 returned to the LS, and it became undetectable for the All-sky Monitor (ASM) onboard the Rossi X-Ray Timing Explorer (RXTE) in May 1999, entering its ‘off’ state, observed before only once with EXOSAT (Ilovaisky et al. 1986). The source was detected with BeppoSAX on 1999 August 13, and its properties were consistent with the off state being a low-luminosity extension of the LS (Méndez & van der Klis 1997; Kong et al. 2000). However, a later observation with BeppoSAX on 2000 September 10 revealed a flux level lower by a factor of ~ 4 than what was detected in 1999 (Corbel et al. 2003). GX 339-4 has remained undetectable by the ASM until 2002. In March 2002, the source became bright again (Smith et al. 2002) and we started an RXTE campaign to follow its evolution. Here we present the results of the timing analysis of a single observation from this campaign, in which a QPO with exceptional behavior was observed. The full spectral/timing analysis from all observations of our campaign will be presented elsewhere. Preliminary results have been reported by Belloni et al. (2002a).

2. Data analysis

Figure 1 shows the 2002/2003 outburst of GX 339-4. The light and color curves are obtained from the data of the Proportional Counter Array (PCA) onboard RXTE. Only counts from the most reliable of the five units of the PCA (PCU2) were used. From the figure it is evident that the outburst had a complex evolution, which can be roughly divided in three parts. In the first part (day 0–34), the count rate increased with time, showing a rather hard spectrum gradually softening with time. The second part (day 34–57, depicted by the gray strip) showed a drop in count rate accompanied by considerable spectral softening. During the third part (day 57–292) the count rate returned almost to the level of the first peak, after which it showed an overall, but sometimes irregular, decay. These changes occurred while the spectrum remained much softer than during the first part of the outburst. From the light curve, it is also clear that variability on a time scale of tens of seconds is much stronger in the spectrally hard part of the outburst. Based on the timing and color data, we conclude that the source evolved from the LS, through the very high state (VHS) or intermediate state (IS), to the HS (Belloni et al. 2002a). A dotted line in Fig. 1 marks the observation discussed in this work.

This observation took place during the transitional phase of the outburst and, although not outstanding in

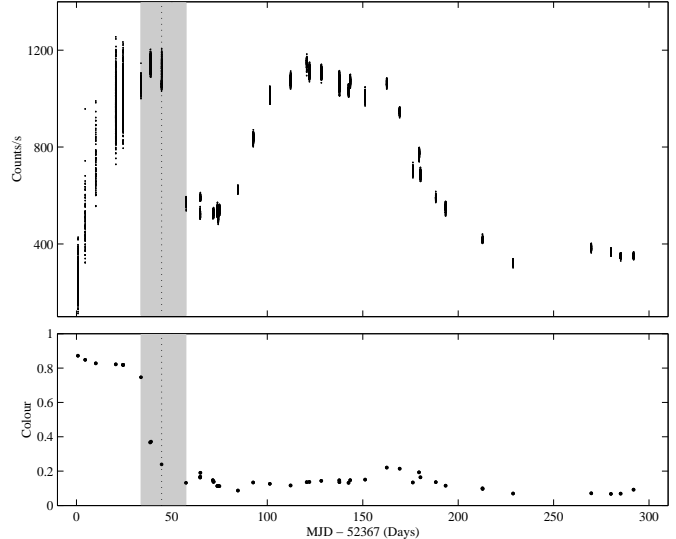


Fig. 1. The 2.9-25.1 keV count rate (top) and color (bottom) evolution of GX 339-4 during its 2002/2003 outburst, as observed with RXTE (PCU2 only). The color is defined as the ratio of counts in the 16.4-19.8 keV band over counts in the 3.7-6.5 keV band. Day 0 corresponds to April 3 2002 (MJD 52367), the vertical dotted line marks the time of the observation analyzed here (May 17 2002/MJD 52411, see Fig. 2 for blow up), and the gray area indicates the transition interval. The time resolution of the light curve is 16s, while in the color curve each point represents a single observation. Data are corrected for background but not for dead time.

the light curve, showed peculiar timing features, different from those observed before and after. It corresponds to 2002 May 17/MJD 52411 (two RXTE orbits, 14:24-14:58 UT and 15:34-16:33 UT), with a total PCA exposure time of 5.58 ks. In Fig. 2 we show a 16-s time resolution light curve and the color evolution during this observation. Below, we present the results of the timing and spectral analysis from these data.

2.1. Power Density Spectra

For the timing analysis, we used **Single bit** data from all active PCUs, with a time resolution of 1.25×10^{-8} s and covering the PCA channel range 0–35, corresponding roughly to 2–16 keV. For each of the two orbits, we subdivided the data into stretches 128 seconds long and produced a power density spectrum (PDS) for each of them. The resulting PDS were then averaged, a logarithmic rebinning was applied, the contribution due to Poissonian statistic was subtracted (Zhang 1995; Zhang et al. 1995), and finally they were converted to fractional squared rms (Belloni & Hasinger 1990). The resulting power density spectra for each orbit are shown in Fig. 3. The two PDS are markedly different. In the first orbit, the power density spectrum shows weak power-law noise with a very broad bump between 6 and 10 Hz. In the second orbit, the power-

law noise is enhanced and a strong QPO at ~ 6 Hz appears, together with its second harmonic. We fitted both power density spectra with a model consisting of Lorentzian components (Miyamoto et al. 1991; Belloni et al. 2002b). During the first orbit, the broad QPO (centroid frequency 7.3 ± 0.2 Hz and full-width at half-maximum 4.4 ± 0.4 Hz) and the continuum noise (consisting of two Lorentzian components) have a fractional rms of $1.73 \pm 0.09\%$ and $1.92 \pm 0.11\%$ respectively. A Lorentzian function proved to be a poor approximation for the strong QPO in the second orbit. This effect has also been observed in a QPO at a similar frequency in XTE J1550-564 (Homan et al. 2001). A good fit to the QPO peak was obtained with a model consisting of a Gaussian plus a broad Lorentzian to account for the extended wings. The centroid frequency of the Gaussian+Lorentzian complex is 5.895 ± 0.004 Hz (the values for the two components are constrained to be the same). The width of the Gaussian is 0.351 ± 0.006 Hz, and the total (Gaussian plus Lorentzian) fractional rms amplitude is $6.68 \pm 0.07\%$. The continuum noise, fitted with two broad Lorentzian components (as for the first orbit), has a total fractional rms of $5.06 \pm 0.08\%$. We repeated the analysis with data at higher energies (PCA channels 36-51, corresponding to 17-24 keV). No signal is detected during the first orbit, although with not very stringent upper limits. During the second orbit, the QPO fractional rms is $17.81 \pm 0.36\%$.

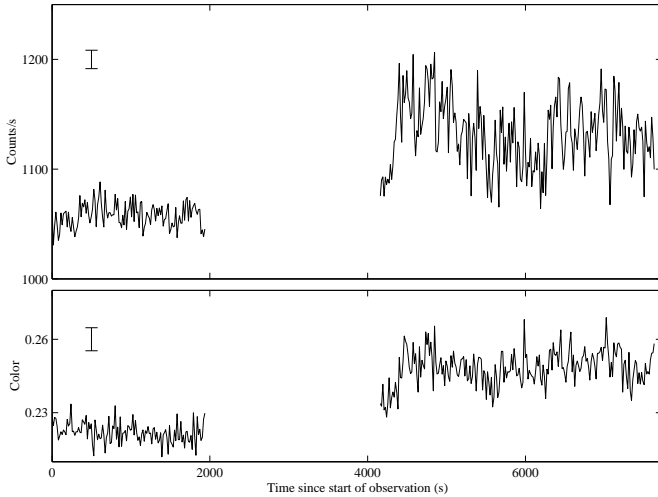


Fig. 2. A blow up of the light and color curve for MJD 52411. Time resolution is now 16s in both curves. Typical error bars are shown. See caption of Fig. 1 for additional details.

2.2. Time-frequency analysis

In order to test whether the inadequacy of the Lorentzian model for the QPO is due to intrinsic variations of its

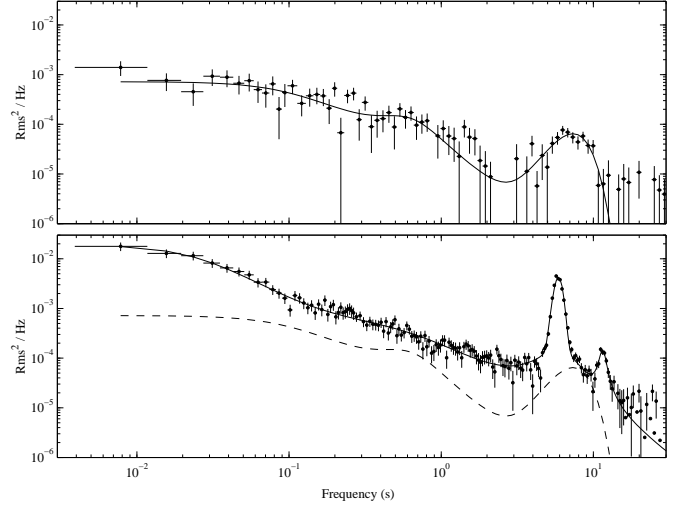


Fig. 3. Power Density Spectra from the two RXTE orbits (top: first orbit; bottom: second orbit). The solid lines correspond to the best-fit models described in the text. For reference, the dashed line in the lower panel shows the best fit of the first orbit.

centroid frequency, we produced a spectrogram, defined (in its continuous version) as

$$S_x(t, \nu) = \left| \int_{-\infty}^{+\infty} x(u) h^*(u - t) e^{-i2\pi\nu u} du \right|^2 \quad (1)$$

Here, $x(t)$ is our signal (PCA channel range 0-35, with a resolution of 128^{-1} s) and $h(t)$ is a window function (in our case, a Welch window of length 4 seconds, see Press et al. 1992). The time step t , which sets the time resolution of the resulting time-frequency image $S_x(t, \nu)$ was chosen to be 1 second. In order to suppress the low-frequency noise, before applying Eqn. 1 we detrended our signal by subtracting from it a spline fit to its 1-s rebinned version. A section of the spectrogram, showing 320 seconds (starting from 50 seconds into the second RXTE orbit) in the frequency range 4-8 Hz is shown in Fig. 4, together with the corresponding light curve (in 1-second bins). Four effects can be observed:

- The QPO is not present in the first 120 seconds of the observation, (we can set a 95% confidence upper limit of 2.1% rms by fitting the PDS of the first 120 s with a QPO with centroid and width fixed to the values reported above), barely visible in the next 20 seconds, and appears clearly only after that (to remain for the rest of the RXTE orbit).
- The light curve shows a net increase in count rate in correspondence with the onset of the oscillation, when also the enhanced low-frequency noise, visible in Fig. 3, turns on.
- The centroid frequency of the QPO shows significant variations in the range 5.5-7.0 Hz.
- The centroid frequency shows a positive correlation with the count rate (shown in the top panel).

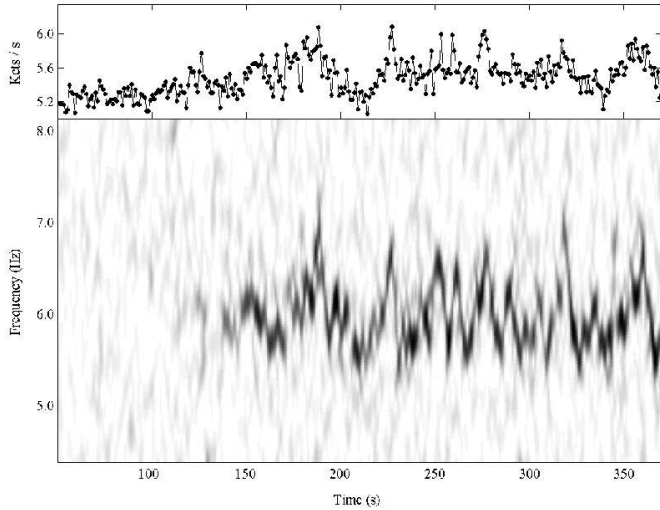


Fig. 4. Top panel: PCA light curve (1 second binning) 50–370 seconds into the second RXTE orbit. Bottom panel: corresponding spectrogram in the 4–8 Hz range; darker regions correspond to higher power.

On the basis of third point we conclude that the shape of the QPO, in particular its broad wings, are indeed the result of the variations in the centroid frequency.

To examine in more detail the QPO-count rate relation, we fitted each power density spectrum in the spectrogram (in the 4–8 Hz range) with a model consisting of a Lorentzian peak and a power law for the local continuum. Visual inspection of the results showed that the model was able to recover accurately the local centroid frequency of the QPO. On average, the FWHM of the best fit Lorentzian was found to be ~ 0.2 Hz. A correlation between QPO frequency and count rate over the entire orbit is clear, although it shows a large scatter.

Since the QPO centroid frequency varies in an irregular way, we produced a PDS of the QPO-frequency time series. In order to avoid problems due to the fact that adjacent Welch windows overlap with each other, introducing a net filtering effect, we repeated the whole analysis with a window length of 2 seconds and non-overlapping windows. The resulting power density spectrum is shown in Fig. 5. A break in the power density spectrum is evident. A fit with a zero-centered Lorentzian yields a characteristic frequency (HWHM) of 0.09 Hz. Fig. 6 shows the correlation between QPO frequency and total count rate from these 2-second windowed data. One can see that there is indeed a correlation between the two quantities, but it is not very strict, with a linear correlation coefficient of ~ 0.5 . Interestingly, the additional noise component below 0.1 Hz in the second orbit, reflects similar time scales as the variations of the QPO frequency.

Although variability properties, such as QPO frequencies, generally correlate better with spectral hardness than with count rate, the statistical quality of our data prevented us from performing a meaningful study with a color instead of count rate.

Table 1. Best fit parameters from the spectral fitting of the data from the two RXTE orbits. Errors correspond to a 1σ confidence range. The total unabsorbed 2–100 keV luminosity was calculated assuming a distance of 4 ± 1 kpc (Zdziarski et al. 1998).

| | Orbit 1 | Orbit 2 |
|----------------------------|----------------------------------|----------------------------------|
| PL Index | 2.44 ± 0.02 | 2.44 ± 0.10 |
| E_c (keV) | 190^{+10}_{-90} | 110^{+70}_{-40} |
| T_{in} (keV) | 0.89 ± 0.01 | 0.92 ± 0.01 |
| E_{line} (keV) | 6.86 ± 0.11 | 6.7 ± 0.2 |
| F_{Tot}^a | $(2.06 \pm 0.06) \times 10^{-8}$ | $(2.25 \pm 0.17) \times 10^{-8}$ |
| F_{disk}^a | $(1.30 \pm 0.04) \times 10^{-8}$ | $(1.18 \pm 0.02) \times 10^{-8}$ |
| F_{pow}^a | $(7.71 \pm 0.35) \times 10^{-9}$ | $(1.02 \pm 0.03) \times 10^{-8}$ |
| L_{tot} (erg s $^{-1}$) | $(3.73 \pm 1.86) \times 10^{37}$ | $(4.07 \pm 2.05) \times 10^{37}$ |

^a unabsorbed 2–100 keV flux (erg cm $^{-2}$ s $^{-1}$)

2.3. Energy spectra

We performed a spectral analysis of the two individual orbits separately, ignoring the first 120 s of the second one. Spectra were created from PCU2 data (2.9–25.2 keV) and HEXTE cluster A data (18.3–150 keV), using the latest version of FTOOLS (5.2). The spectra were corrected for background and dead time effects, and fitted with XSPEC 11.2 using a model consisting of a cutoff power law (**cutoff**), a disk black body (**diskbb**), an accretion disk line (**laor**) and a smeared edge (**smedge**). The interstellar absorption N_H was fixed to a value of 5×10^{21} atoms/cm 2 (Ilovaisky et al. 1986). For both orbits, good fits were obtained. The fit parameters were consistent between the two orbits (see Table 1). The only differences were found in the fluxes of the disk black body and of the cutoff power law: while the first decreased by 9%, the second increased by more than 30%, resulting in an overall hardening of the spectrum. The calculated fluxes in the 2 – 100 keV range for the two RXTE orbits are reported in Table 1.

3. Discussion

We have discovered a strong transient 6 Hz QPO in GX 339–4 with some unusual properties: a sharp turn-on in time and large frequency variability on a typical time scale of ~ 10 seconds. The QPO was found in an observation that was performed during a transition from a hard to a soft state, during which the spectral and variability properties were those typical for a Very High State. It is interesting to note that, while the observation occurred during a transition from a hard to a soft spectral state, the appearance of the QPO in our observation is associated with the hardening of the energy spectrum. This indicates that such a hard to soft transition is not a smooth process throughout the outburst.

The sharp 6 Hz QPO in the second orbit turned on within ~ 20 seconds, similar to the timescale of the sharp increase observed in the light curve. While a broad QPO was present during the first part of our observation, it is

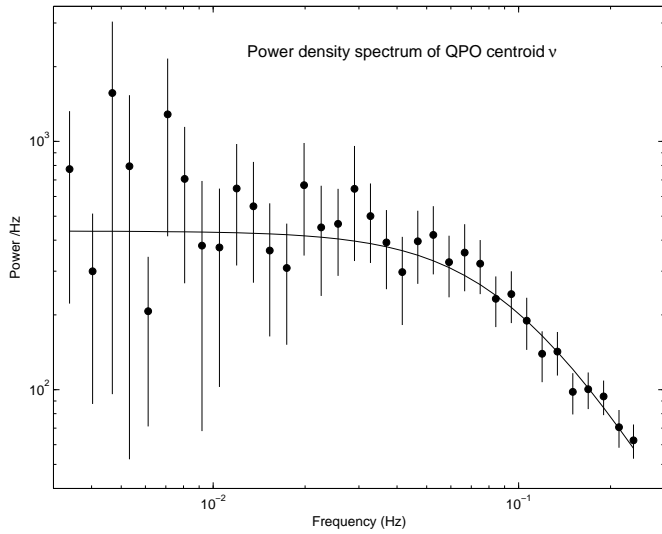


Fig. 5. Power Density Spectrum of the QPO centroid frequency (see text). Power is in units of Hz^2 . The line is a best fit with a zero-centered Lorentzian model.

not clear whether the 6 Hz QPO evolved from this broad feature; the former is much weaker, less coherent, and peaks at a different frequency. We note that in case the broad feature is still present in the second part of the observation, it might be partly responsible for the asymmetric wings of the 6 Hz QPO (see Fig. 3). Such ‘shoulders’ have been reported before for similar 6 Hz QPOs in other BHCs. In the terminology introduced by Wijnands et al. (1999) and Remillard et al. (2002b) for QPOs in XTE J1550-564, the peak in the first orbit could be interpreted as a type A QPO, and the ones in the second orbit as type B; the observed spectral hardening is consistent with this interpretation. Besides the changes around 6–7 Hz, also the continuum at lower frequencies shows considerable changes. As noted before, the increase in power below 0.1 Hz might reflect the count rate variations that correlate with the changes in the QPO frequency that have a similar time scale (see Fig. 6).

The observed FWHM of ~ 0.2 Hz in the dynamical power spectrum is consistent with being solely due to smearing by frequency changes. This sets a lower limit to the Q value of the QPO of ~ 30 , indicating a signal lifetime of at least 5 s. The fact that we see uninterrupted frequency changes of 10 seconds and more suggests a longer lifetime. If we associate the observed frequency with a certain radius in the disk, it is unlikely that the QPO is caused by a single blob of matter, as the blob would have to move inward and outward. It is possible that what we observe is the result of different blobs that appear and live at slightly different radii, which vary on a similar time scale. However, Fig. 4 and Fig. 5 show that the QPO frequency variations are not consistent with a white noise, i.e. there is a correlation between the QPO frequencies at different times. This would mean that each new blob would “know” about the previous ones. In a model like that of Psaltis & Norman (2003), where a particular ac-

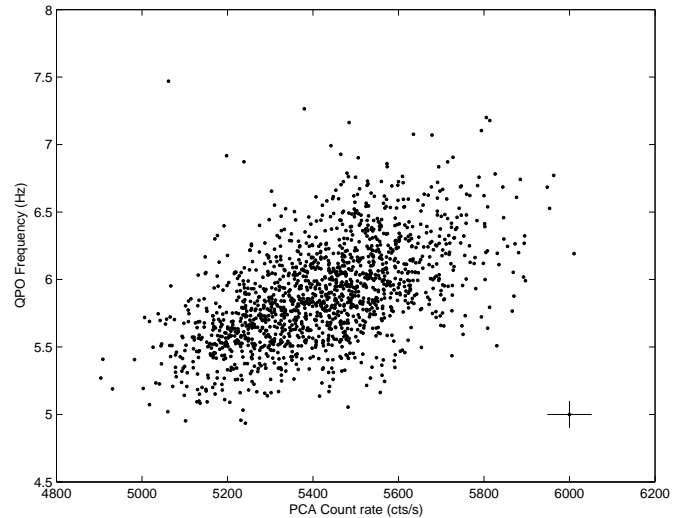


Fig. 6. QPO frequency vs. PCA count rate for the 2-s binned data (see text). Typical error bars are shown.

cretion disk radius acts as a band-pass filter, the observed variations would translate into corresponding variations of this filtering radius, resulting in a natural correlation between different frequencies at different times. The observed count-rate/frequency correlation would then suggest a relation between this filtering radius and the X-ray flux.

Given its peculiarities, one might wonder whether this QPO detection is unique. A similar sharp QPO peak, needing a Gaussian model for a satisfactory fit, was found by Homan et al. (2001) in the black-hole transient XTE J1550-564. This QPO (defined as type B by Homan et al. 2001) was also detected in a few observations with a centroid frequency around 6 Hz. A sub-harmonic and two higher harmonics were also detected. Interestingly, a similar sharp QPO was observed in the Ginga data of the transient GS 1124-68 (Miyamoto et al. 1994; Belloni et al. 1997). Takizawa et al. (1997) classify the QPOs observed in GS 1124-68 into two separate classes: the sharp QPO peak was only observed in the range 5–7 Hz, similar to what we detected in our data. Homan et al. (2001) also report the sudden appearance of a QPO in XTE J1550-564 associated to a count rate increase. However, in this case the X-ray colors indicate a small and gradual softening of the spectrum. A sharp QPO around 6 Hz, with harmonic and sub-harmonic components and a similar low-frequency noise, was found by Cui et al. (2000) in the transient XTE J1859+226. A narrow peak was present in three of the four observations analyzed, with a centroid frequency around 5.96 Hz, with properties similar to those seen in our data. Another narrow QPO peak was found in the bright transient GRS 1739-27, although at 5 Hz (Wijnands et al. 2001). The QPO, with its first overtone, was observed in the second part of the data and not in the first part, where only a weak noise component at low frequencies was noticed. Wijnands et al. (2001) found that the frequency of the QPO increased together with the

count rate, with an even better correlation with the hard color. All these QPOs have a centroid frequency of 5-7 Hz. It is not clear, however, why the same frequency should play the same role in different systems. In all these cases, the QPO is associated to a VHS-like energy spectrum, with the presence of both a hard and a soft component, has a fractional rms of a few percent and a FWHM similar to that shown here. In order not to vary too much over systems with black holes of different masses, the dependence of its frequency with mass of the central object must be weak.

The QPO observed here shows, moreover, characteristics in common with both the HBO and the NBO of NS LMXB (see van der Klis 1995), letting open the question if a stronger connection can be established either with one or the other feature. HBOs present LFN (Low Frequency Noise), with rms of 1-8 %, the oscillation has a frequency that correlates with count rate and an rms of 2-8 %, the spectrum is hard. NBOs show VLFN (Very Low Frequency Noise), with a rms of 0.6-4 %, no LFN, the frequency of the oscillation varies between 5 and 7 Hz, and its rms is 1-3 %, while the energy spectrum is hard. Nothing can be said about correlation between count rate and frequency over short time scale.

The rapid count-rate increase observed in our observation, corresponding to a hardening of the flux, shows similarities to the “dips” and “flip-flops” reported by Miyamoto et al. (1991) from GX 339-4 and by Takizawa et al. (1997) from GS 1124-68, although the time scale of our transition is slower. In both cases, GX 339-4 and GS 1124-68, a QPO peak was observed only in the high-flux intervals, similar to our data, although the continuum noise was stronger at low flux, contrary to what we observe here. The corresponding spectral variations were similar to ours: the flux increase was caused by a 30% increase of the hard component, while the disk component did not vary. The spectral parameters remained unchanged (Miyamoto et al. 1991). Notice that also in GS 1124-68, the centroid frequency of the sharp QPO is positively correlated with count rate (Takizawa et al. 1997).

The spectral hardening observed in connection to the appearance of the QPO suggests that the oscillation is associated to the hard spectral component, as it is usually observed for low-frequency QPOs. However, the presence of a soft component seems to be necessary for the observation of such a QPO, as one can see also in the cases of XTE J1550-564, GS 1124-68 and XTE 1859+226. A QPO with these characteristics (narrow, around 6 Hz and with a weak noise component) seems to be always associated to a sort of “intermediate” spectral state, when both spectral components are present (see e.g. Rutledge et al. 1999).

The results showed here pose constraints to theoretical models for the production of the QPO. A successful model should be able to reproduce a sharp appearance of a QPO like the one we observe, but also the rapid variability of the characteristic frequency of the oscillation (see Fig. 5) should be explained.

Acknowledgements. TB thanks the Cariplo Foundation for financial support. JH acknowledges support from Cofin-2000 grant MM02C71842.

References

- Alpar, M. A. & Shaham, J. 1985, *Nature*, 316, 239
- Belloni, T. & Hasinger, G. 1990, *A&A*, 227, L33
- Belloni, T., Méndez, M., van der Klis, M., Lewin, W. H. G., & Dieters, S. 1999, *ApJ*, 519, L159
- Belloni, T., Nespoli, E., Homan, J., et al. 2002a, in “New Views on Microquasars”, Eds. P. Durouchoux, Y. Fuchs, J. Rodriguez, Centre For Space Physics, Kolkata, p75
- Belloni, T., Psaltis, D., & van der Klis, M. 2002b, *ApJ*, 572, 392
- Belloni, T., van der Klis, M., Lewin, W. H. G., et al. 1997, *A&A*, 322, 857
- Corbel, S., Nowak, M. A., Fender, R. P., Tzioumis, A. K., & Markoff, S. 2003, *A&A*, 400, 1007
- Cui, W., Shrader, C. R., Haswell, C. A., & Hynes, R. I. 2000, *ApJ*, 535, L123
- Homan, J., Wijnands, R., van der Klis, M., et al. 2001, *ApJS*, 132, 377
- Hynes, R. I., Steeghs, D., Casares, J., Charles, P. A., & O’Brien, K. 2003, *ApJ*, 583, L95
- Ilovaisky, S. A., Chevalier, C., Motch, C., & Chiappetti, L. 1986, *A&A*, 164, 67
- Kong, A. K. H., Kuulkers, E., Charles, P. A., & Homer, L. 2000, *MNRAS*, 312, L49
- Maejima, Y., Makishima, K., Matsuoka, M., et al. 1984, *ApJ*, 285, 712
- Méndez, M. & van der Klis, M. 1997, *ApJ*, 479, 926
- Miller, M. C., Lamb, F. K., & Psaltis, D. 1998, *ApJ*, 508, 791
- Miyamoto, S., Kimura, K., Kitamoto, S., Dotani, T., & Ebisawa, K. 1991, *ApJ*, 383, 784
- Miyamoto, S., Kitamoto, S., Iga, S., Hayashida, K., & Terada, K. 1994, *ApJ*, 435, 398
- Nowak, M. A. 2002, in “New Views on Microquasars”, Eds. P. Durouchoux, Y. Fuchs, J. Rodriguez, Centre For Space Physics, Kolkata, p3
- Press, W. H., Teukolsky, S. A., Vetterling, W. T., & Flannery, B. P. 1992, *Numerical recipes in FORTRAN. The art of scientific computing* (Cambridge: University Press, 1992, 2nd ed.)
- Psaltis, D. & Norman, C. 2003, *ApJ*, in press, (astro-ph/0001391)
- Remillard, R., Munro, M., McClintock, J. E., & Orosz, J. 2002a, in “New Views on Microquasars”, Eds. P. Durouchoux, Y. Fuchs, J. Rodriguez, Centre For Space Physics, Kolkata, p49
- Remillard, R. A., Sobczak, G. J., Munro, M. P., & McClintock, J. E. 2002b, *ApJ*, 564, 962
- Rutledge, R. E., Lewin, W. H. G., van der Klis, M., et al. 1999, *ApJS*, 124, 265
- Smith, D. M., Swank, J. H., Heindl, W. A., & Remillard, R. A. 2002, *The Astronomer’s Telegram*, #85, 85, 1
- Stella, L. & Vietri, M. 1998, *ApJ*, 492, L59

- Strohmayer, T. E., Zhang, W., Swank, J. H., et al. 1996, ApJ, 469, L9
- Takizawa, M., Dotani, T., Mitsuda, K., et al. 1997, ApJ, 489, 272
- Tanaka, Y. & Lewin, W. H. G. 1995, in X-ray binaries (Cambridge Astrophysics Series, Cambridge, MA: Cambridge University Press, 1995, edited by Lewin, Walter H.G.; Van Paradijs, Jan; Van den Heuvel, Edward P.J.), p. 126
- van der Klis, M. 1995, in X-ray binaries (Cambridge Astrophysics Series, Cambridge, MA: Cambridge University Press, 1995, edited by Lewin, Walter H.G.; Van Paradijs, Jan; Van den Heuvel, Edward P.J.), p. 252
- Wijnands, R., Homan, J., & van der Klis, M. 1999, ApJ, 526, 33
- Wijnands, R., Méndez, M., Miller, J. M., & Homan, J. 2001, MNRAS, 328, 451
- Zdziarski, A. A., Poutanen, J., Mikolajewska, J., et al. 1998, MNRAS, 301, 435
- Zhang, W. 1995, XTE/PCA Internal Memo
- Zhang, W., Jahoda, K., Swank, J. H., Morgan, E. H., & Giles, A. B. 1995, ApJ, 449, 930